

AD-A065 358

AD

AD-E400 278

TECHNICAL REPORT ARPAD-TR-77005

A SEMI-AUTOMATIC RADIOGRAPHIC METHOD FOR
DETECTING FELT PADS AND FIBER SEALS IN
TANK AMMUNITION

JOSEPH M. ARGENTO
EMMETT G. BARNES

TECHNICAL
LIBRARY

JANUARY 1979



US ARMY ARMAMENT RESEARCH AND DEVELOPMENT COMMAND
PRODUCT ASSURANCE DIRECTORATE
DOVER, NEW JERSEY

APPROVED FOR PUBLIC RELEASE; DISTRIBUTION UNLIMITED.

The views, opinions, and/or findings contained in this report are those of the author(s) and should not be construed as an official Department of the Army position, policy or decision, unless so designated by other documentation.

Destroy this report when no longer needed. Do not return to the originator.

The citation in this report of the names of commercial firms or commercially available products or services does not constitute official endorsement or approval of such commercial firms, products, or services by the United States Government.

UNCLASSIFIED

SECURITY CLASSIFICATION OF THIS PAGE (When Data Entered)

SECURITY CLASSIFICATION OF THIS PAGE(When Data Entered)

SECURITY CLASSIFICATION OF THIS PAGE(When Data Entered)

TABLE OF CONTENTS

	<u>Page No.</u>
Introduction	1
Procedures	2
Analysis	3
Recommendations	5
Distribution List	13
 Tables	
1 Radiographic technique	6
2 Differences in density from normalization point	6
3 Differences in density from normalization (seals)	7
4 Calculations	7
5 Comparison of film density measurements: component present vs component missing	8
 Figures	
1 Scan of felt pad at 0°	9
2 Scan of seal at 0° orientation	10
3 Scan of washer at 0°	11

INTRODUCTION

Radiographic nondestructive testing is used to inspect M393 105 mm HEP-T projectiles to assure the integrity of the explosive charge and the proper assembly of the components. Conventional techniques are employed in which images are formed on radiographic film and are read and interpreted by human inspectors. These radiographs have sufficient contrast to show the presence or absence of wax impregnated felt pads, felt washers, and fiber seals in the assembly, providing the radiographic exposures are carefully controlled and reference radiographs showing both defective and acceptable conditions are used for comparison. The importance of these components, and the difficulty and subjectivity of visual interpretation, required that the feasibility be investigated for developing an instrumented inspection method of automatically determining the presence or absence of the components in assembled projectiles.

Experiments were done with the Joyce-Loebl scanning microdensitometer on film radiographs of M393 HEP-T projectiles. These radiographs were scanned to determine whether a semi-automated film reading system could be designed to find the presence of the felt pad, felt washer, and seal in the shell, and whether this could be accomplished using the same film used for the explosive and assembly inspection.

Three shells representing different conditions were supplied for these experiments. Shell number one had a wax-impregnated pad and washer and contained a seal. Shell two was without the pad, washer and seal. Shell three contained a pad, washer, and seal, but the pad and washer were free of wax. The shells were identical in all other important respects.

After radiographing the three shells in various orientations, the films were scanned using the microdensitometer, and density curves were developed for the areas of interest. The data collected from the curves were compiled and analyzed. There is a distinct difference in film density between the waxed pad and washer and the no-pad, no-washer conditions and between the seal and no-seal conditions. Finally, we conclude that a relatively simple semi-automated system can probably be designed to read the film and determine whether or not the shell contains the felt pad, felt washer and seal.

PROCEDURES

The three sample shells were radiographed on the one million volt G.E. unit in the ARRADCOM radiographic facility. The alignment was carefully controlled to minimize parallax. This was especially important in the seal area, because a slight misalignment there would make it impossible to position the film on the densitometer accurately. This orientation was arbitrarily called the 0° position. The shells were then turned in 30° increments and radiographed until they reached 150° . This procedure was followed to ensure that defects could be detected in arbitrary orientations, and to provide films representing the density fluctuations that normally occur due to slight drifts in exposure and processing conditions. A total of six radiographs containing 18 individual shell images was produced.

Each developed film was placed on the microdensitometer and scanned. Table 1 lists the radiographic technique and microdensitometer settings. Density curves from which the data in tables 2 and 3 are derived were generated by the microdensitometer. After the cycle of scans was completed, a calibrated step wedge was placed on the 0° graphs so that the density range that the densitometer was measuring could be determined. These densities are indicated on the 0° graphs, and are adjusted to the same base line as curve number 1. The 0° graphs are shown in figures 1, 2, and 3.

To cull data from the graphs, three curves for a particular orientation and specific part (i.e., felt pad, washer or seal) were drawn on the same paper. The three graphs represent the three conditions that are found in the sample shell. On the 0° orientation felt pad graph, curve 1 is the waxed felt pad, curve 2 is no pad, and curve 3 is the unwaxed pad. This particular labelling is used throughout and is summarized as follows:

1 = waxed felt pad, waxed washer, seal

2 = no felt pad, no washer, no seal

3 = felt pad, washer, seal.

The curves were normalized by slipping the base lines of curves 2 and 3 to match curve 1, so that the point lying at the extreme right of each curve was at the same place on the density scale. This yields a simple graphic representation of the differences between the three conditions. Since the film densities of corresponding points on all radiographs used in this study fall within a fairly narrow range of values, a particular physical density change or thickness variation in a projectile can be assumed to produce the same film density change on all radiographs. Using the calibrated stepwedge, indications of the density differences between this normalization point and other points on the curves could be read directly. The slight differences in base line in

original radiographs and the normalization procedure mean that the absolute optical density measurements from the graph are valid for curve 1, but not for curves 2 or 3.

Positioning the film on the densitometer so that points lying along the same vertical line on the graphs would correspond to equivalent points on the radiographs was also a problem. Placing several radiographs on the densitometer in sequence in exactly the same location is nearly impossible. Therefore, characteristic points along the curves were chosen on the assumption that these points would correspond to identical points on the radiographs and within the shell. The minimum (highest density) was chosen for the felt pad and washer. The inflection point at which the curve began its steep ascent (toward lower density) was chosen for the seal. Differences in density were then computed from the normalization point to these characteristic points. Lower densities are toward the top of the graph for convenience.

ANALYSIS

Having collected this information, a rudimentary analysis was carried out. The mean, variance, and standard deviation were calculated:

$$y = \frac{\sum_i y_i}{N} ;$$

$$\text{variance} = \frac{\sum_i (y_i)^2}{N} - \frac{(\sum_i y_i)^2}{N^2} ;$$

$$\text{standard deviation} = \sqrt{\frac{N}{N-1} \text{variance.}}$$

where N = number of data points and y_i is the value of the i th data point. These calculations are summarized in table 4.

The data show that the density difference between the felt pads with wax and no pad at all is greater than a single density increment on the stepwedge. This implies that the detection of the missing pad is possible using instrumentation of comparable accuracy and precision. This follows not only from the density difference but also from the fact that information was derived from different radiographs with inherent differences in exposures and processing. The same conclusions can be drawn for the presence or absence of the waxed felt washer. Although the data for the seal area was more difficult to obtain, we can say that the detection of no seal is possible.

The differences in density between the plain pad and no pad is significantly less than the differences between the waxed pad and no pad showing that the quantitative detection of the absence of an unwaxed felt pad would be more difficult. Therefore, we suggest that the felt pad and washer be wax impregnated to optimize detection. This may require additional quality controls on the manufacture of the pads and washers. The seal does not contain wax, nor is it needed for detection.

The calculated values in table 4 can be further analyzed by establishing the component-missing condition as a new base line and noting the difference from the component-present condition. Table 5 shows that the .319 density difference between the no-pad and waxed pad-present conditions constitutes a separation of better than 20 standard deviations. The separation for the waxed washer is over 6 standard deviations. Certainly these values constitute a substantial quantitative difference and support the feasibility of determining a missing pad condition by some automated means. The problem of bringing the process up to the required speed should not present a major obstacle, since only a few points on each radiograph need to be sampled.

The criteria for determining whether the radiographs are amenable to computer analysis can be summarized as follows:

1. Definable structures exist within the radiograph. For example, the felt pad area is substantially darker than the surrounding area. It is rectangular and easily located.
2. There are specific relationships between areas of the radiograph. For example, the felt washer and felt pad have a spacial relationship to each other on every radiograph and at all orientations.
3. Size, area or density differences exist in the radiograph. This was measured in the experiment. There was a definite, reproducible difference between the densities of selected features on the film.
4. The information is quantifiable. Standard mathematical definitions exist for film density. It does not appear to take unduly long to compute the densities from basic light intensity measurements.
5. The data can be accumulated, analyzed, and graphed as points with error bars. A histogram of optical density and a more elaborate statistical analysis can be developed.
6. Density readings taken directly from the film appear to be adequate for this application.
7. Fiducial marks on the film such as the edge of the felt pad area, the edge of the seal and the washer area can be used to align the film by hand.

8. There is a constant structure from radiograph to radiograph. This entails careful monitoring of the alignment of shell, the processing of the film and the positioning of film on the film reader at the production plant so that numbers derived from the film can be analyzed and compared with other data.

The constancy of structure among the radiographs depended upon the careful manual screening of radiographs before they were submitted for felt pad or washer determination. Normalization points lie within the area of the explosive charge, and any film density increase caused by voids in the explosive rendered density measurements at these points invalid. In developing and implementing an automated system, a choice would have to be made either to continue the manual pre-screening (possibly during the normal explosive inspection) or to select new density reference points on the radiographs which would not be subject to shell-to-shell variations. Our reference (normalization) points were chosen only for the convenient use of the scanning microdensitometer and its data format, and it should be possible to identify a number of other valid points.

CONCLUSIONS

Determining the presence or absence of felt pads, washers, and fiber seals in this particular situation lends itself to automation in the sense that the computer will measure and decide whether the shell is defective or not. It will be semi-automated because the film radiograph will be aligned by hand. Several point reading densitometers could be placed in a regular array, so that when the film was placed over them and positioned properly the felt pad, washer and seal would be aligned with some of the instruments. The remaining densitometers would be positioned to measure regions that would give the normalization for this particular film. The digitized information would then be fed to a microcomputer, where the decision as to the acceptability of the shell could be made. It is possible to envisage other designs incorporating television, flying spot scanners, or other devices. The selection of an optimum technique and system configuration will require additional engineering studies.

RECOMMENDATIONS

It is recommended that the felt pads and washers be impregnated with wax to optimize detection. This may require additional quality controls on the manufacture of the pads and washers. The seal does not contain wax, nor is it needed for detection.

It is recommended that additional engineering studies be made to select the optimum technique and system configuration.

Table 1. Radiographic technique

Equipment: G.E. 1000 Resotron ("reflected" beam used)
 X-ray Energy: 950 kv
 Beam Current: 1.1 ma
 Film: Kodak AA
 Radiographic Screens: Lead metal; .030 in front, .010 in back
 Exposure Time: 2 $\frac{1}{4}$ min (speed 10 on rotating carousel)
 Film-to-source Distance: 6 ft
 Film Processing: Kodak x-omat, model A

Microdensitometer Settings

Equipment: Joyce-Loebl model MK3 CS (MDM 2)
 Objective Lens: Bausch-Lomb 48 mm /.08
 Slit Width: .2 mm
 Proportional Control: Felt pad, Washer 5
 Fiber Seal 8
 Feedback Setting: 5
 Wedge Range: Felt Pads and Washers: 0-1
 Fiber Seal: 0-5
 Ratio Arm: 20:1

Table 2. Differences in density from normalization point

Shell Orientation	Felt Pad*			Felt Washer*		
	1-Waxed Pad	2-No Pad	3-Plain Pad	1-Waxed Washer	2-No Washer	3-Plain Washer
0°	.163333	.45500	.279222	.069003	.328649	.207973
30°	.132222	.451111	.264833	.058091	.325439	.26125
60°	.151278	.453056	.284667	.048142	.247449	.233970
90°	.147778	.466278	.280	.044932	.312601	.208615
120°	.144667	.471333	.288944	.0308108	.315490	.234611
150°	.119389	.476389	.307222	.019257	.374544	.221132

*Data taken at minimum of each curve (maximum optical density).

Table 3. Differences in density from normalization (seals)

Orientation	Seal*		
	1-Seal Present	2-No Seal	3-Seal Present
0°	1.0165	1.6967	1.2217
30°	0.959	1.672	1.102
60°	1.1533	1.881	1.1647
90°	1.2027	1.8069	1.349
120°	1.121	1.5751	1.2502
150°	1.3243	1.9475	1.3585

*Inflection point used as arbitrary registration point for measurements. The inflection point is the point at which the curve begins a steep ascent (toward lower optical density).

Table 4. Calculations

	Mean density difference	Variance	Standard deviation
Felt Pad			
1	.143111	.000197	.015370
2	.462195	.000093	.010581
3	.284148	.000162	.013930
Felt Washer			
1	.0450393	.000270	.018008
2	.317362	.001396	.040930
3	.227925	.000335	.018298
Seal			
1	1.12947	.014972	.130983
2	1.7632	.016312	.139910
3	1.24102	.008512	.101064

Table 5. Comparison of film density measurements:
component present vs. component missing

	Density Difference*	Number of Standard Deviations Difference*
Waxed Felt Pad Present	.319	20.7
Plain Felt Pad Present	.178	12.8
Waxed Felt Washer Present	.272	6.6
Plain Felt Washer Present	.0895	2.2
Fiber Seal Present	.634	4.5

*Differences taken between the mean for the condition indicated and the corresponding component missing condition, as shown in table 4.

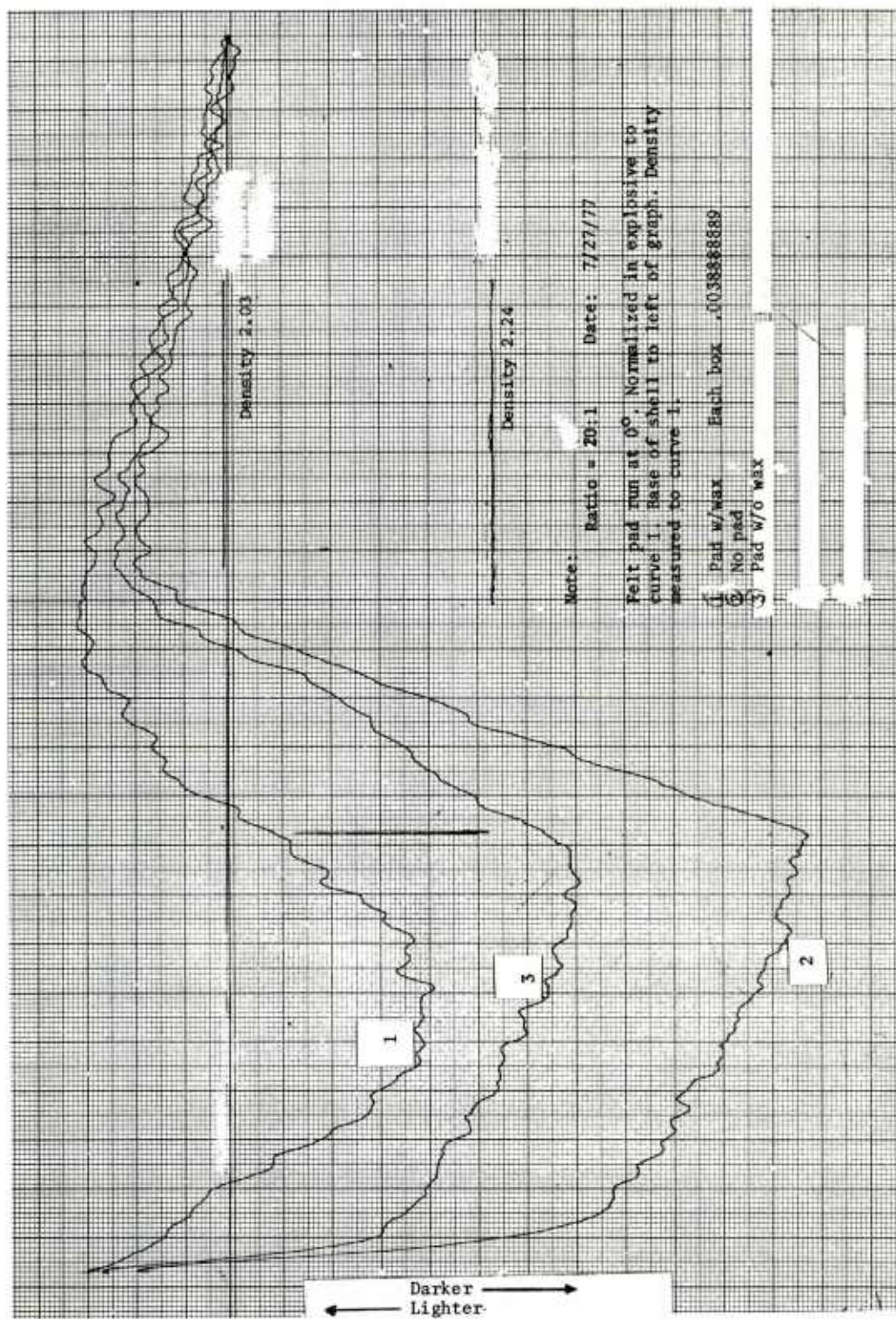


Figure 1. Scan of felt pad at 0°.

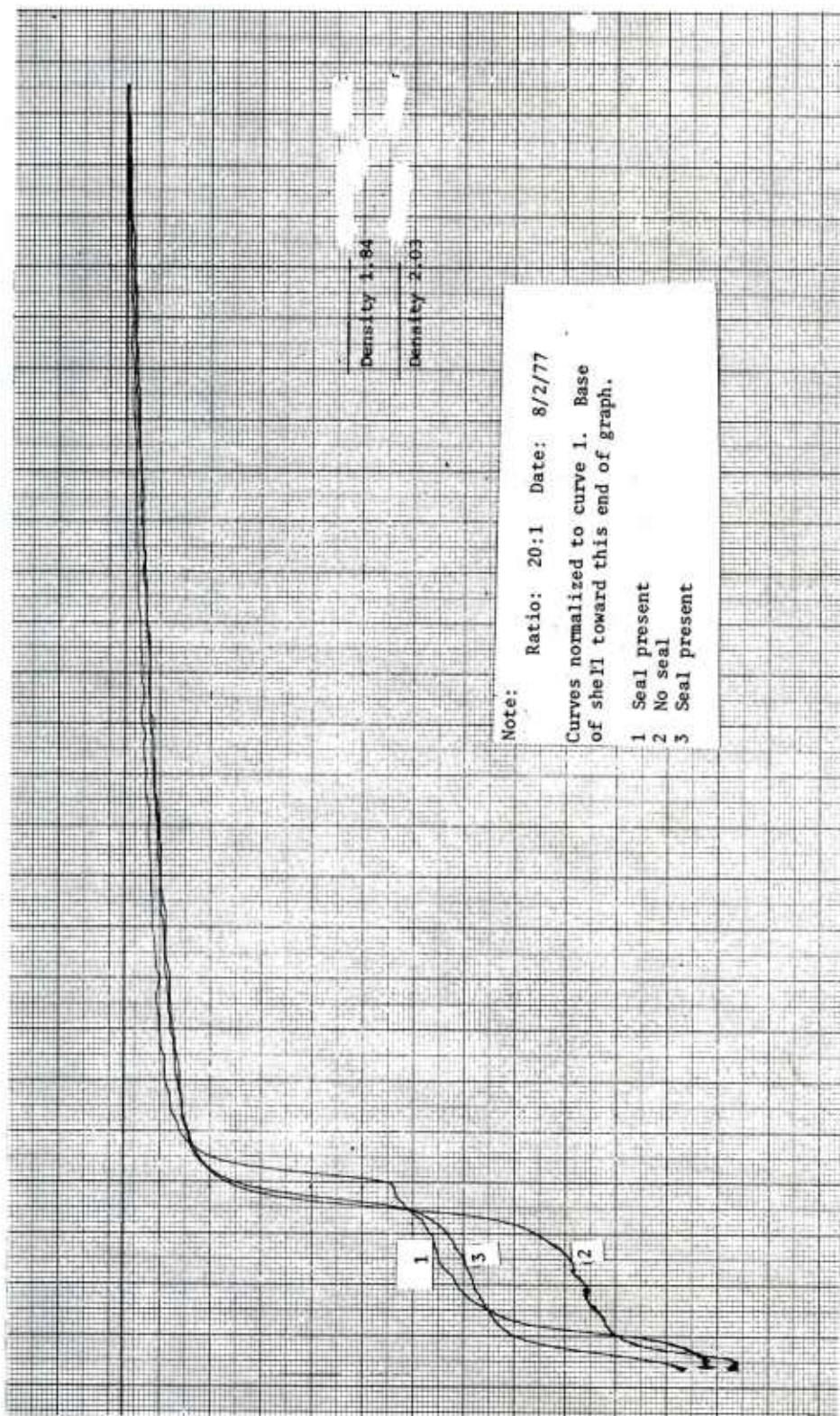


Figure 2. Scan of seal at 0° orientation.

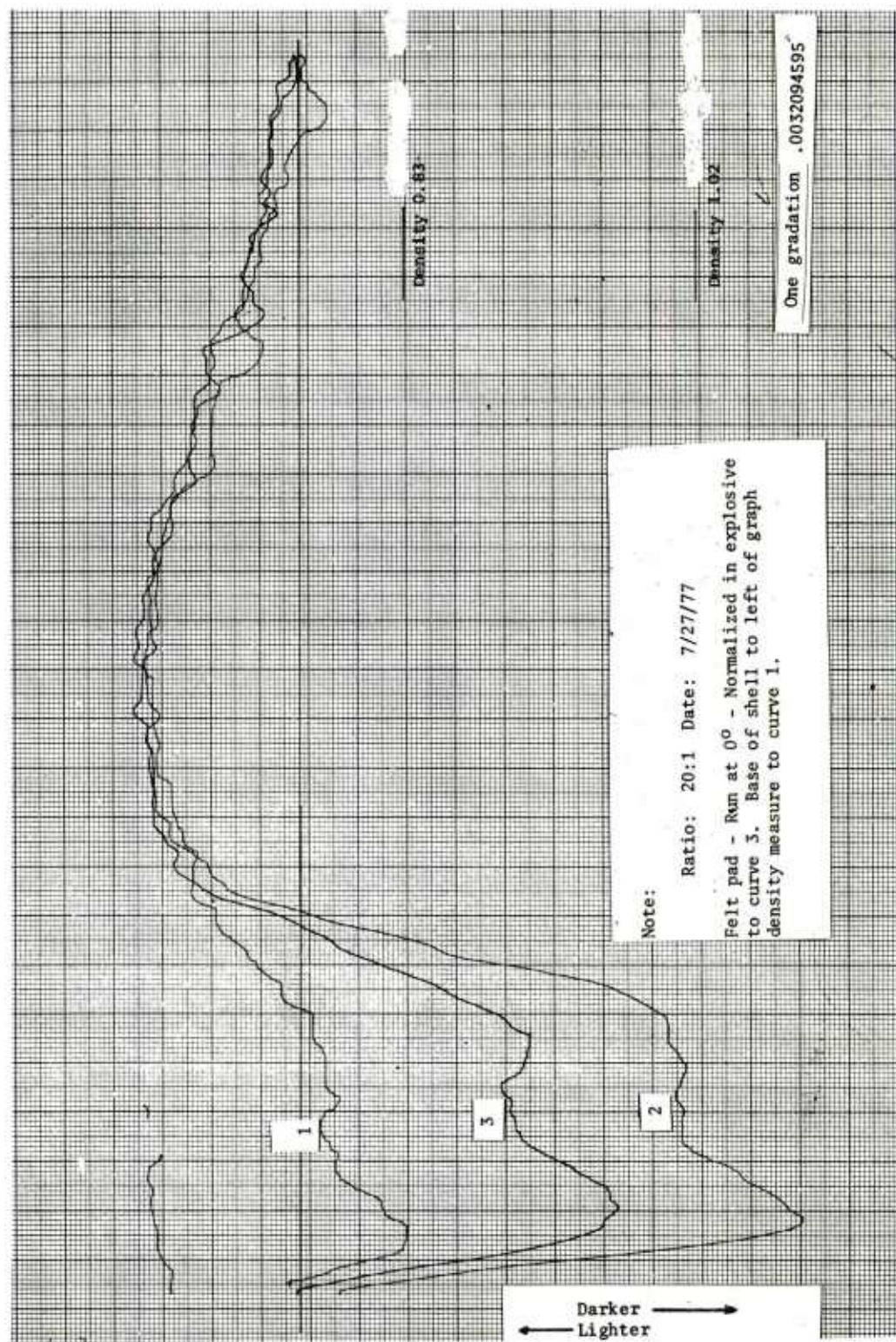


Figure 3. Scan of washer at 0° .

DISTRIBUTION LIST

Commander

U.S. Army Armament Research and Development Command
ATTN: DRDAR-QAS (5)
DRDAR-QAR (5)
DRDAR-QAN (5)
DRDAR-TSS (5)
Dover, NJ 07801

Defense Documentation Center (12)
Cameron Station
Alexandria, VA 22314

U.S. Army Armament Materiel Readiness Command
ATTN: DRSAR-LEP-L
Rock Island, IL 61299

Director

U.S. Army TRADOC Systems Analysis Activity
ATTN: ATAA-SL (Tech Library)
White Sands Missile Range, NM 88002

Weapon System Concept Team/CSL
ATTN: DRDAR-ACW
Aberdeen Proving Ground, MD 21010

Technical Library
ATTN: DRDAR-CLJ-L
Aberdeen Proving Ground, MD 21005

Technical Library
ATTN: DRDAR-TSB-S
Aberdeen Proving Ground, MD 21010

Technical Library
ATTN: DRDAR-LCB-TL
Benet Weapons Laboratory
Watervliet, NY 12189

U.S. Army Materiel Systems Analysis Activity
ATTN: DRXSY-MP
Aberdeen Proving Ground, MD 21005